© 2017. Published by The Company of Biologists Ltd | Journal of Cell Science (2017) 130, 2893-2902 doi:10.1242/jcs.203844

RESEARCH ARTICLE

Microscopy analysis of reconstituted COPII coat polymerization and Sec16 dynamics

Hirohiko Iwasaki, Tomohiro Yorimitsu and Ken Sato*

ABSTRACT

The COPII coat and the small GTPase Sar1 mediate protein export from the endoplasmic reticulum (ER) via specialized domains known as the ER exit sites. The peripheral ER protein Sec16 has been proposed to organize ER exit sites. However, it remains unclear how these molecules drive COPII coat polymerization. Here, we characterized the spatiotemporal relationships between the *Saccharomyces cerevisiae* COPII components during their polymerization by performing fluorescence microscopy of an artificial planar membrane. We demonstrated that Sar1 dissociates from the membrane shortly after the COPII coat recruitment, and Sar1 is then no longer required for the COPII coat to bind to the membrane. Furthermore, we found that Sec16 is incorporated within the COPII–cargo clusters, and that this is dependent on the Sar1 GTPase cycle. These data show how Sar1 drives the polymerization of COPII coat and how Sec16 is spatially distributed during COPII coat polymerization.

KEY WORDS: COPII, Sar1, Small GTPase, Sec16

INTRODUCTION

The endoplasmic reticulum (ER) is responsible for the biogenesis of most secretory and membrane proteins. The COPII coat complex mediates the formation of transport carriers that bud from the ER and traffic proteins and lipids to the Golgi (Barlowe and Miller, 2013; D'Arcangelo et al., 2013). The COPII coat consists of an inner layer of the Sec23–Sec24 heterodimeric complex surrounded by an outer layer of the Sec13–Sec31 heterotetramer complex, and these components are sequentially assembled onto the ER membrane through the action of the small GTPase Sar1 to generate COPII-coated transport carriers (Barlowe et al., 1994). In brief, assembly of the COPII coat is triggered by GDP/GTP exchange on Sar1 (Nakano and Muramatsu, 1989) catalyzed by the ER-resident guanine nucleotide exchange factor (GEF) Sec12 (Barlowe and Schekman, 1993). The binding of GTP induces a conformational change in Sar1 allowing association with the ER membrane (Huang et al., 2001; Bi et al., 2002). Membrane-associated Sar1-GTP recruits the Sec23–Sec24 complex by binding to the Sec23 subunit, whereas the Sec24 subunit captures the cargo protein to form a prebudding complex (Miller et al., 2002, 2003; Mossessova et al., 2003). The Sec23 subunit is the GTPase-activating protein (GAP) for Sar1 and therefore stimulates Sar1 GTP hydrolysis upon prebudding complex formation, resulting in dissociation of the Sec23 subunit from Sar1 (Yoshihisa et al., 1993; Antonny et al., 2001). However, even in the presence of ongoing GTP hydrolysis, the membrane association of Sec23–Sec24 is stabilized through the interaction of the Sec24 subunit with transmembrane cargo and repeated cycles of Sec12-dependent GTP loading of Sar1, which facilitates proper and efficient cargo sorting into COPII vesicles (Sato and Nakano, 2005b). Subsequently, the prebudding complex recruits the Sec13–Sec31 complex, which polymerizes adjacent prebudding complexes to drive membrane deformation and vesicle budding (Bi et al., 2007; Tabata et al., 2009).

The molecular organization of the COPII coat components and their order of assembly on the membrane have been described in detail through crystallographic studies (Bi et al., 2002, 2007; Fath et al., 2007) and *in vitro* reconstitution assays (Oka et al., 1991; Barlowe et al., 1994; Matsuoka et al., 1998; Antonny et al., 2001). However, the spatiotemporal dynamics of each COPII component during their assembly has not been clearly defined. The size of the COPII-coated bud (60–80 nm in diameter), below the spatial resolution of conventional light microscopy, has made it difficult to assess how the COPII components are mutually organized in the course of their assembly. Furthermore, COPII vesicles appear to arise from specialized regions of the ER known as ER exit sites (ERES) (Orci et al., 1991; Bannykh et al., 1996; Budnik and Stephens, 2009), and the conserved large hydrophilic protein Sec16 has been described as the organizer of the ERES (Connerly et al., 2005; Watson et al., 2006; Bhattacharyya and Glick, 2007; Ivan et al., 2008; Hughes et al., 2009). Recent studies from our and other groups have suggested that the GTPase inhibitory activity mediated by Sec16 modulates the assembly of the COPII coat at ERES (Kung et al., 2012; Yorimitsu and Sato, 2012). Although Sec16 has been shown to associate with multiple COPII coat subunits and Sar1 (Gimeno et al., 1996; Shaywitz et al., 1997; Yorimitsu and Sato, 2012), the spatiotemporal distribution in the context of COPII coat dynamics is poorly understood.

As reported previously, we have been able to reconstitute fluorescently labeled transmembrane cargo proteins into a horizontal planar lipid bilayer, allowing the spatiotemporal dynamics of the cargo molecules induced by the minimal COPII machinery to be visualized by total internal reflection fluorescence (TIRF) microscopy (Tabata et al., 2009) (Fig. 1A). In this system, the vesicle release from the planar membrane is arrested in order to observe the COPII vesicle bud immediately before the vesicle pinch-off. To achieve this, we use a relatively thick planar membrane in comparison to the physiological membrane thickness. The COPII components can collect cargo molecules in such a thick membrane but cannot induce vesicle pinch-off. Furthermore, under the above condition, longer incubation induces lateral polymerization of the COPII coat and allows formation of micron-sized flattened COPII-driven cargo clusters in the membrane that are visible by TIRF microscopy (Tabata et al., 2009) (Fig. 1B). Therefore, this system is

Department of Life Sciences, Graduate School of Arts and Sciences, University of Tokyo, Komaba, Meguro-ku, Tokyo 153-8902, Japan.

*Author for correspondence (kensato@bio.c.u-tokyo.ac.jp)

H.I., 0000-0003-1552-7369; K.S., 0000-0002-1858-6236

Received 9 March 2017; Accepted 14 July 2017

Journal of Cell Science (2017) 130, 2893-2902 doi:10.1242/jcs.203844

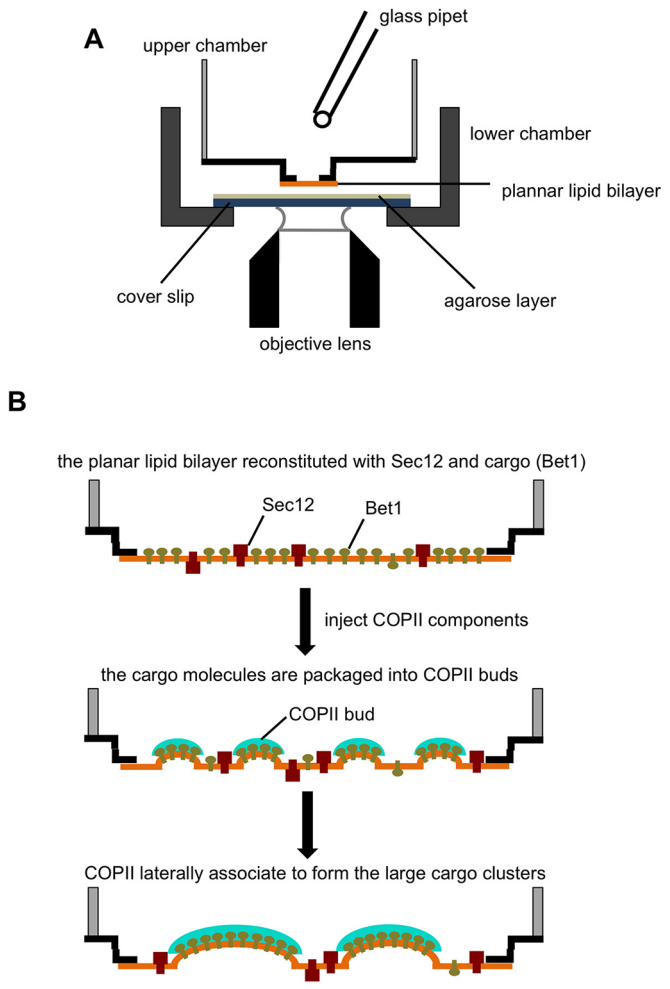

Fig. 1. Lateral polymerization of the COPII coat and formation of micron-sized flattened COPII–cargo clusters. (A) Overview of the horizontal planar lipid bilayer formation apparatus. The apparatus consists of an upper chamber and a lower chamber. On the bottom of the upper chamber, a thin plastic film with a small hole (100–150 µm) was attached and an artificial planar lipid bilayer was formed horizontally across the hole on an agarose-coated coverslip. The upper chamber could be moved vertically using a micromanipulator. (B) Schematic illustration of the process where COPII-driven cargo clusters are formed in the membrane.

well suited to obtain a spatial overview of how the COPII coat polymerization proceeds. Here, by using this system, we clarified several key features regarding the molecular dynamics of the *Saccharomyces cerevisiae* COPII coat, Sar1, Sec12 and Sec16 during their assembly.

RESULTS

Distribution of Sar1 during COPII–cargo cluster formation

To gain insights into the spatiotemporal correlation between the individual COPII components during their assembly, we reconstituted both Bet1 (an ER-to-Golgi SNARE as a model cargo) and Sec12Δlum (Sec12 without its luminal domain, but containing the transmembrane region) in the 'vesicle pinch-off-deficient' planar lipid bilayer and added COPII coat components (Sec23–Sec24 and Sec13–Sec31) and Sar1 to generate COPII–cargo clusters. Unless otherwise stated, reconstituted membrane as described above was used in all experiments and all proteins are from *S. cerevisiae*. For each fluorescently labeled target protein, we observed and analyzed the dynamic behavior by fluorescence microscopy. We used dual-color confocal microscopy to examine the distribution of COPII components relative to Bet1 cargo clusters, and TIRF microscopy was used for a more detailed quantitative analysis because of its high *z*-axis resolution.

COPII coat assembly can be minimally reconstituted on synthetic liposomes (Matsuoka et al., 1998) or cargo-reconstituted proteoliposomes (Sato and Nakano, 2004) by using Sec23–Sec24, Sec13–Sec31, and GTP-locked Sar1 with the non-hydrolyzable GTP analog, GMP-PNP. Therefore, we first observed the dynamics of fluorescently labeled Sar1 (Sar1–Cy3) during COPII assembly under this minimal condition by TIRF microscopy. The addition of the COPII coat and Sar1–Cy3 in the presence of GMP-PNP yielded various sizes of fluorescent clusters (Fig. 2A, upper panel). These clusters are likely to represent COPII-mediated Bet1 clusters associated with GTP-locked Sar1–Cy3. The Bet1 clusters largely overlapped with the distribution of Sar1 when their colocalizations were analyzed by dual-color confocal microscopy be observing mCherry-fused Sar1 (Sar1–mCherry), which was confirmed to retain the Sec23-mediated GTPase activity, together with Bet1 labeled with DyLight488 (Bet1–Dy488) (Fig. 2C, upper panels).

For a better overview of the cluster profiles obtained from TIRF microscopy, we divided the clusters into large (>1.0 µm^2) and small (<1.0 µm^2) clusters, and determined the distribution of the average fluorescence intensities of these clusters (Fig. 2D). We found no significant difference in the average fluorescence intensity between large and small clusters, confirming that small clusters grow laterally or coalesce to form larger clusters. The line-scan profile of fluorescence intensity across a typical cluster showed that Sar1–Cy3 molecules were evenly distributed within the cluster (Fig. 2A, lower panel). Moreover, the distribution of the average fluorescence intensities of these clusters fitted well with a single Gaussian distribution (Fig. 2E). These results corroborate that the observed clusters arise from a specific association of Sar1–Cy3 with the assembled cargo instead of a random aggregation of the Sar1–Cy3 proteins.

We next examined the behavior of Sar1 in the presence of GTP instead of GMP-PNP. Although GTP hydrolysis by Sar1 causes its dissociation from the membrane (Antonny et al., 2001), we have shown previously that the membrane association of COPII subunits can be maintained by interactions with transmembrane cargo proteins and continual GTP loading of Sar1 by Sec12 (Sato and Nakano, 2005b). However, the assembly dynamics of COPII coat proteins in relation to Sar1 association/dissociation remains unclear. To address this, we first analyzed the dynamics of Sar1–mCherry together with the dynamics of Bet1–Dy488 using confocal microscopy. Notably, Sar1–mCherry was found to predominantly distribute along the distal edge of the Bet1–Dy488 clusters and not throughout the clusters as observed with GMP-PNP (Fig. 2C, lower panels). When Sar1–Cy3 molecules were visualized in the presence of GTP by TIRF microscopy, the addition of the COPII components yielded clusters of various sizes as observed in the presence of GMP-PNP (Fig. 2A, upper panel). A line-scan of Sar1–Cy3 fluorescence taken across a representative image of a Sar1–Cy3-containing cluster obtained from TIRF microscopy demonstrated that peaks in Sar1–Cy3 fluorescence are in a ring at the edge of the cluster (Fig. 2A, lower panel). When the fluorescence signal intensity was measured along the perimeter of a typical cluster and plotted as a function of pixel position, Sar1–Cy3 was observed to distribute homogeneously along the edge regions surrounding the cargo clusters (Fig. 2B). We observed no clear differences in average fluorescence intensities between large (>1.0 µm^2) and small

Journal of Cell Science (2017) 130, 2893-2902 doi:10.1242/jcs.203844

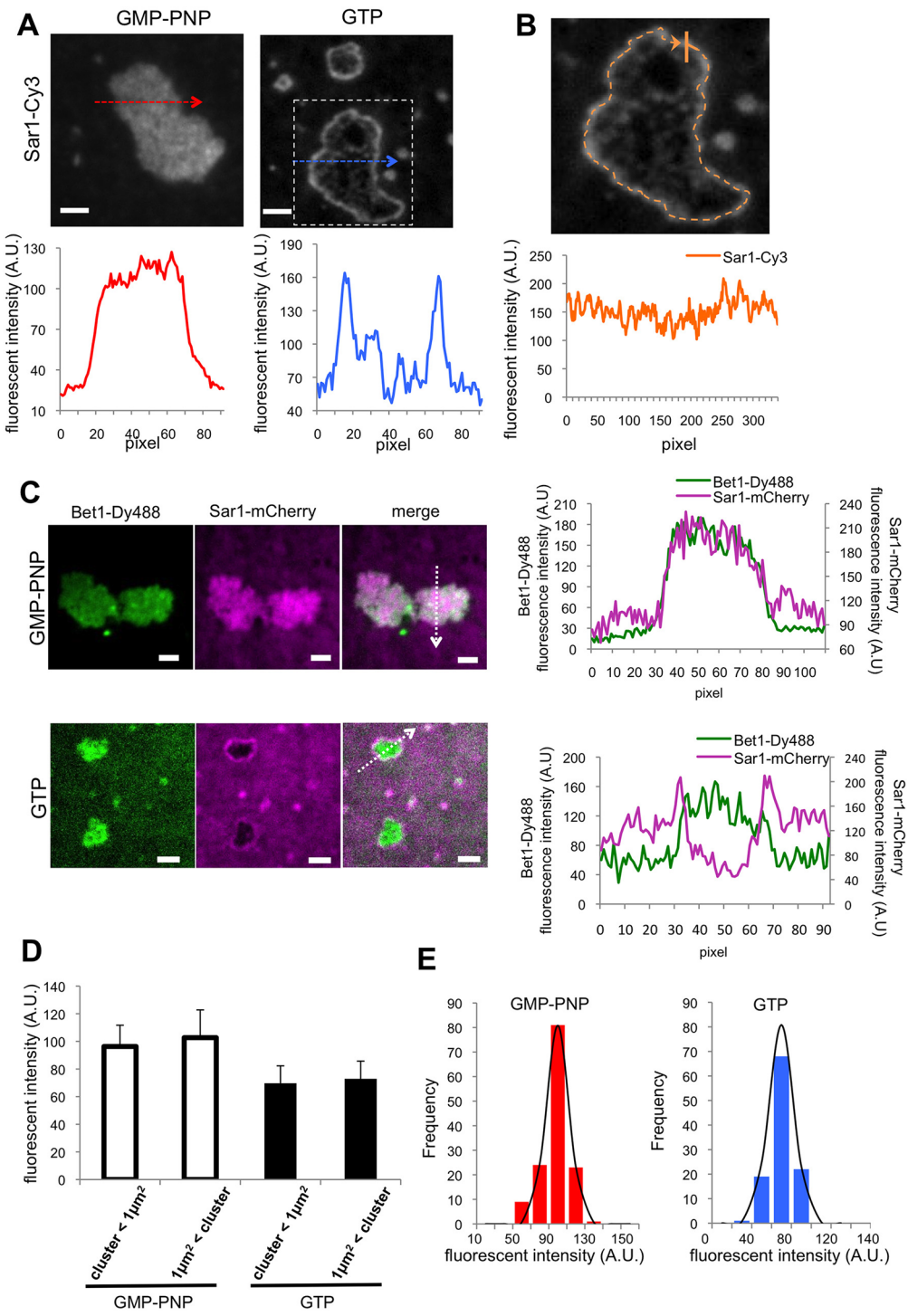

Fig. 2. COPII-induced Sar1 assembly in the bilayer membrane. (A) COPII components (80 ng Sar1–Cy3, 640 ng Sec23–Sec24 and 1.3 µg Sec13–Sec31) were added from the upper chamber to the membrane reconstituted with Bet1 and Sec12Δlum. Upper panels show fluorescence images of Sar1–Cy3 in the cluster formed in the presence of GMP-PNP or GTP. Fluorescence images were taken under a TIRF microscope. Data shown were taken from representative clusters. Lower panels show the line-scan quantification of the fluorescent signal at the position indicated by the dashed arrow in upper panels. (B) Magnified image of the region outlined by the dashed box in A. A line-scan (dashed orange arrow in upper panel) along the cluster perimeter measures fluorescence intensity of Sar1–Cy3 (lower panel). (C) The colocalization of Bet1–Dy488 and Sar1–mCherry in the clusters formed in the presence of GMP-PNP or GTP. COPII components (39 ng Sar1–mCherry, 380 ng Sec23–Sec24 and 1.3 µg Sec13–Sec31) were added to the membrane reconstituted with Bet1–Dy488 and Sec12Δlum. Fluorescence images were taken under a confocal microscope. Dy488 and mCherry fluorescence channels and merged images are shown. Right panels show the line-scan quantification of the fluorescent signal at the position indicated by the dashed arrow in the merged images. (D) Normalized average fluorescence intensity of Sar1–Cy3 in the large clusters (>1 µm^2) compared to the small clusters (<1 µm^2). Fluorescence from each cluster was normalized to background fluorescence. Error bars represent s.e.m. (GMP-PNP: cluster <1 µm^2, n=100; cluster >1 µm^2, n=18; GTP: cluster <1 µm^2, n=94; cluster >1 µm^2, n=16). (E) Distribution of the normalized average fluorescence intensity of Sar1–Cy3 in the clusters (A.U., arbitrary units) observed in A in the presence of GMP-PNP or GTP. Histograms of the fluorescence intensity were fitted to a single Gaussian distribution (lines). Scale bars: 2 µm.

(<1.0 µm^2) clusters (Fig. 2D), and the distribution of the average fluorescence intensities of these clusters fitted well with a single Gaussian distribution (Fig. 2E). These results confirm that the observed GTP-driven clusters are not simply the result of the Sar1–Cy3 aggregation. We found that the average fluorescence intensity (per pixel area) of the Sar1–Cy3 in the clusters was slightly lower when the cluster formation was carried out with GTP (70.2±12.6 AU) than with GMP-PNP (97.3±16.3 AU) (Fig. 2D). This result may reflect the continuous cycle of Sar1–Cy3 binding and dissociation. Considering that the membrane association of Sar1 is a prerequisite for COPII coat recruitment, these results suggest that coat recruitment and polymerization occur at the edge region of a cargo cluster. Furthermore, Sar1 is likely to dissociate from the membrane immediately after the COPII recruitment and their lateral association.

Sar1 is not required to maintain the COPII–cargo cluster

Sar1 is considered to serve as an anchor for the COPII coat; hence, these results prompted the question as to whether the COPII coat is still present in the center region of the cluster. To assess this, we labeled the outer layer of the COPII coat subcomplex Sec13–Sec31 with Cy3 (Sec13/31–Cy3) and observed the distribution in the

Journal of Cell Science (2017) 130, 2893-2902 doi:10.1242/jcs.203844

clusters. Sec13/31–Cy3 was confirmed to retain its Sec23 GAP stimulation activity. We found that Sec13/31–Cy3 is present throughout the clusters in the presence of GMP-PNP and even under GTP-hydrolyzing conditions (Fig. 3A, upper panels). These clusters most likely represent COPII–cargo clusters because ATTORho101-labeled Sec13–Sec31 (Sec13/31–ATTORho101)

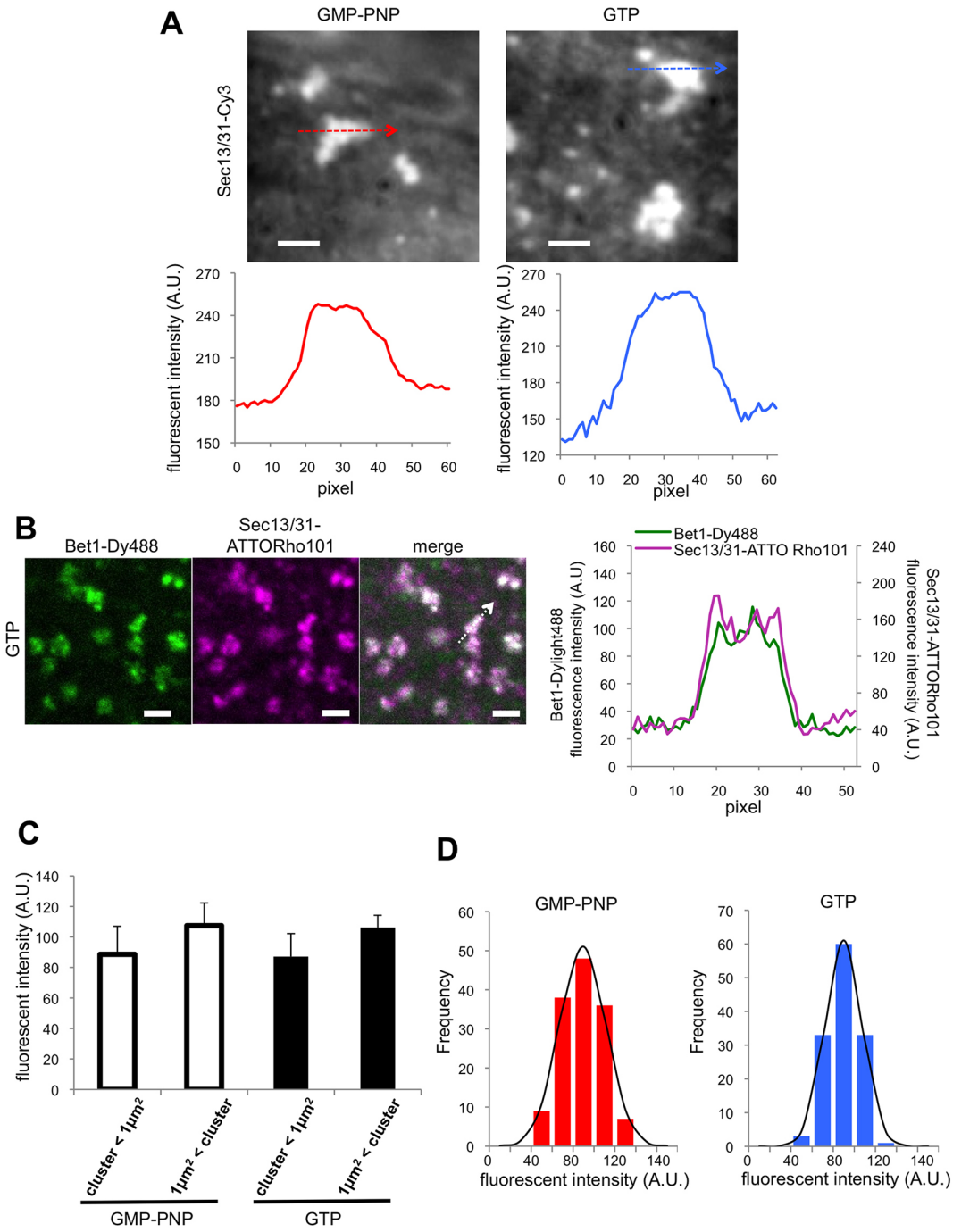

Fig. 3. Distribution of Sec13–Sec31 within the COPII–cargo cluster. (A) COPII components (100 ng Sar1, 640 ng Sec23–Sec24 and 1.65 µg Sec13/31–Cy3) were added to the membrane reconstituted with Bet1 and Sec12Δlum. Upper panels show fluorescence images of Sec13/31-Cy3 in the cluster formed in the presence of GMP-PNP or GTP. Fluorescence images were taken under a TIRF microscope. Data shown were taken from representative clusters. Lower panels show the line-scan quantification of the fluorescent signal at the position indicated by the dashed arrow in upper panels. (B) The colocalization of Bet1–Dy488 and Sec13/31–ATTORho101 in the clusters formed in the presence of GTP. COPII components (100 ng Sar1, 380 ng Sec23–Sec24, 970 ng Sec13–Sec31 and 240 ng Sec13/31–ATTORho101) were added to the membrane reconstituted with Bet1–Dy488 and Sec12Δlum. Fluorescence images were taken under a confocal microscope. Dy488 and ATTORho101 fluorescence channels, and merged images are shown. Right panel shows a line-scan quantification of the fluorescent signal at the position indicated by the dashed arrow in the merged image. (C) Normalized average fluorescence intensity of Sec13/31–Cy3 in the large clusters (>1 µm^2) compared to the small clusters (<1 µm^2). Fluorescence from each cluster was normalized to background fluorescence. Error bars represent s.e.m. (GMP-PNP: cluster <1 µm^2, n=133, cluster >1 µm^2, n=6; GTP: cluster <1 µm^2, n=122; cluster >1 µm^2, n=11). (D) Distribution of the normalized average fluorescence intensity of Sec13/31–Cy3 (A.U., arbitrary units) in the clusters observed in A in the presence of GMP-PNP or GTP. Histograms of the fluorescence intensity were fitted to a single Gaussian distribution (lines). Scale bars: 2 µm.

Journal of Cell Science (2017) 130, 2893-2902 doi:10.1242/jcs.203844

clusters largely overlapped with the distribution of Bet1–Dy488 (Fig. 3B). It is noteworthy that these Bet1 clusters did not grow to a larger size as observed in Fig. 2 when Sec13/31–Cy3 or Sec13/31–ATTORho101 was used. We presume that this is likely an artifact of the chemical labeling of Sec13–Sec31 with fluorescent tags.

The fluorescence distribution of Sec13/31–Cy3 within the cluster was relatively homogeneous as supported by the line-scan data (Fig. 3A, lower panels). The average fluorescence intensities of the large (>1.0 μm^2) and small (<1.0 μm^2) Sec13/31-Cy3-labeled clusters showed no significant difference (Fig. 3C), and their distribution fitted well with a single Gaussian distribution, in both the presence of GTP and of GMP-PNP (Fig. 3D). These results again confirmed that the observed clusters arise from specific associations of Sec13/31–Cy3 on the membrane instead of a random aggregation of the Sec13/31–Cy3 proteins. Moreover, these data also show that once the COPII coat is assembled into a polymeric lattice on the membrane, Sar1 is no longer required for the COPII coat to adhere to the membrane. We failed to observe the cluster formation when Sec23/24 labeled with a fluorescent protein was used, even though Sec23/24 fused to fluorescent protein has been shown to retain its biological activity both *in vitro* (Sato and Nakano, 2005b) and *in vivo* (Shindiapina and Barlowe, 2010; Iwasaki et al., 2015). This is most likely due to steric hindrance caused by the bulky fluorescent protein attached to Sec23/24, which may interfere with the ability of the Sec23/24 coat to laterally associate to form the flattened large COPII–cargo clusters.

The non-cargo protein Sec12 is excluded from the COPII–cargo cluster

Because the membrane recruitment of Sar1 requires an interaction with its GEF Sec12 (Barlowe and Schekman, 1993), the observed Sar1 distribution in the presence of GTP raised the question as to whether Sec12 is also concentrated along the edge of the clusters. To address this, we fused Sec12Δlum tagged with mOrange (mOrange–Sec12) and examined its distribution within the membrane in relation to the COPII–cargo clusters. As shown in Fig. 4A, the addition of the COPII components yielded clusters observed as dark contrasting regions exhibiting relatively low levels of fluorescent signals. These dark clusters are considered to represent unlabeled COPII–cargo clusters, as evident in a merged image of mCherry-fused Sec12Δlum (mCherry–Sec12) and Bet1–Dy488 obtained by confocal microscopy (Fig. 4B). The mOrange-/mCherry-fused Sec12Δlum proteins were confirmed to be enzymatically active, as assessed by the *in vitro* Sar1 GEF assays. We observed no significant concentration of Sec12 along the edge of the Bet1 clusters, and Sec12 was found to localize primarily in the external regions of the cargo clusters (Fig. 4A,B). The density of mOrange–Sec12 included in the COPII–cargo clusters was significantly lower than that observed outside the clusters as shown by the line-scan analysis of a representative region, indicating that Sec12 is efficiently excluded from COPII–cargo clusters (Fig. 4A,B). The exclusion was not significantly affected by either the presence of GMP-PNP (67.2±4.0%, mean±s.e.m., of background fluorescence) or GTP (67.8±7.3% of background fluorescence) (Fig. 4C). We have shown previously that the non-cargo membrane protein Ufe1 can be efficiently excluded from cargo clusters, and that the efficiency of exclusion is dependent on the Sar1 GTPase cycle (Tabata et al., 2009). To directly compare the relative exclusion efficiency of Ufe1 versus Sec12, we fused MBP–Ufe1 (Sato and Nakano, 2004) with GFP (GFP–Ufe1) and examined its distribution relative to mCherry–Sec12 within the COPII–cargo clusters. Indeed, the exclusion of GFP–Ufe1 was less effective than that of mCherry–Sec12 (GFP:mCherry signal ratio of 2.81±0.39) in the presence of GMP-PNP, whereas it was as effective as that of mCherry–Sec12 (GFP:mCherry signal ratio of 1.31±0.19) in the presence of GTP (Fig. 4D,E). These results indicate that the minimal COPII machinery mediates exclusion of Sec12 from the COPII–cargo clusters, and that, unlike for other non-cargo membrane proteins such as Ufe1, the process of exclusion does not require the Sar1 GTPase cycle.

The behavior of Sec16 during COPII–cargo cluster formation

Sec16 has been shown to be essential for the biogenesis of ERES by interacting with COPII coat subunits and Sar1 (Espenshade et al., 1995; Gimeno et al., 1996; Shaywitz et al., 1997; Connerly et al., 2005; Yorimitsu and Sato, 2012). We have previously shown that fluorescently labeled Sec16 alone can self-assemble into homo-oligomeric complexes on a planar lipid membrane (Yorimitsu and Sato, 2012). However, the spatiotemporal relationship between COPII components and Sec16 during their assembly remains to be characterized. To elucidate this relationship, we used dual-color confocal microscopy to examine the distribution of fluorescently labeled Sec16 (Sec16–mCherry) relative to COPII–cargo clusters (Bet1–Dy488). Purified Sec16–mCherry was confirmed to have an inhibitory effect on the ability of Sec31 to stimulate Sec23 GAP activity. The addition of the complete set of COPII components with Sec16–mCherry to the membrane preloaded with GTP yielded cargo clusters (Fig. 5A). A merged image of Bet1–Dy488 and Sec16–mCherry showed that these clusters seem to incorporate Sec16–mCherry. These results suggest that the oligomeric complexes of COPII–cargo clusters specifically incorporate Sec16.

We next tested the distribution of Sec16–mCherry in relation to COPII components in the presence of GMP-PNP to observe the effect of the Sar1 GTPase cycle on Sec16 behavior. Upon addition of the complete set of COPII components and Sec16–mCherry with GMP-PNP to the membrane, the incorporation of Sec16 into the COPII–cargo clusters was less effective than with GTP (Fig. 5B, upper panels). Instead, the clusters marked by Bet1–Dy488 were relatively devoid of Sec16–mCherry signal compared with the background (70.4±5.7% of background fluorescence). To verify this result, we further used Sar1–Dy488 instead of Bet1–Dy488 to visualize the COPII clusters. Similarly, a reduced extent of Sec16–mCherry incorporation (66.8±7.9% of background fluorescence) into the COPII–cargo clusters was observed with GMP-PNP (Fig. 5B, lower panels). These data suggest that the incorporation of Sec16 into the fully assembled COPII coat requires the Sar1 GTPase cycle and indicate that the result shown in Fig. 5A is not a consequence of nonspecific binding of Sec16 to COPII components. Furthermore, when Sec16–mCherry was added exogenously to preformed COPII–cargo (Bet1–Dy488) clusters in the presence of GTP, less incorporation of Sec16–mCherry was observed (Fig. 5C). Sec16 was found to localize along the edge of the cargo clusters as observed with Sar1-GTP in Fig. 2. These results further confirm that the incorporation of Sec16 into the COPII–cargo clusters is not a result of nonspecific interactions between Sec16 and COPII components. Additionally, these results provide evidence that the incorporation of Sec16 is closely associated with the ongoing Sar1 GTPase cycle.

DISCUSSION

We described a qualitative fluorescence imaging approach to assess how the COPII components and Sec16 are spatiotemporally organized during their assembly. Our use of a planar lipid bilayer system combined with fluorescence imaging enables us to visualize

Journal of Cell Science (2017) 130, 2893-2902 doi:10.1242/jcs.203844

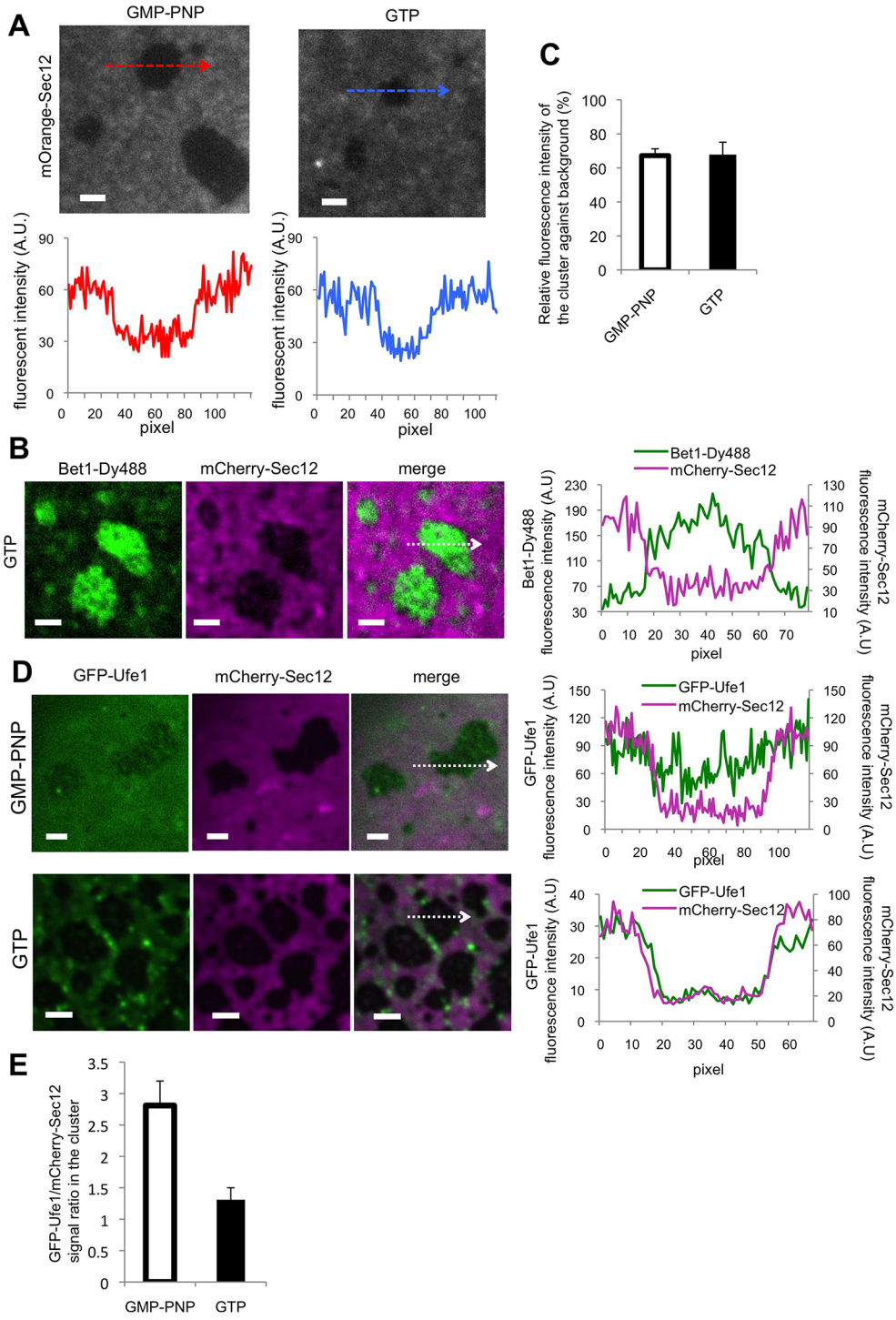

Fig. 4. Distribution of Sec12 during COPII–cargo cluster formation. (A) COPII components (100 ng Sar1, 640 ng Sec23–Sec24 and 1.3 µg Sec13–Sec31) were added to the membrane reconstituted with Bet1 and mOrange–Sec12. Upper panels show fluorescence images of mOrange–Sec12 after COPII–cargo cluster formation in the presence of GMP-PNP or GTP. Fluorescence images were taken under a TIRF microscope. Data shown were taken from representative images. Lower panels show the line-scan quantification of the fluorescent signal at the position indicated by the dashed arrow in upper panels. (B) The colocalization of Bet1–Dy488 and Sec12–mCherry in the clusters formed in the presence of GTP. COPII components (100 ng Sar1, 380 ng Sec23–Sec24 and 1.3 µg Sec13–Sec31) were added to the membrane reconstituted with Bet1–Dy488 and mCherry–Sec12. Fluorescence images were taken under a confocal microscope. Dy488 and mCherry fluorescence channels, and merged images are shown. The right panel shows the line-scan quantification of the fluorescence signal at the position indicated by the dashed arrow in the merged image. (C) The relative density of mOrange–Sec12 in the clusters compared to that outside the cluster. Results are mean±s.e.m. (GMP-PNP, n=9; GTP, n=8). (D) The colocalization of GFP–Ufe1 and mCherry–Sec12 in the clusters formed in the presence of GMP-PNP or GTP. COPII components (100 ng Sar1, 345 ng Sec23–Sec24, and 1.3 µg Sec13–Sec31) were added to the membrane reconstituted with Bet1, GFP-Ufe1, and mCherry-Sec12. Fluorescence images were taken under a confocal microscope. The GFP and mCherry fluorescence channels and the merged images are shown. The right panel shows a line-scan quantification of the fluorescent signal at the position indicated by the dashed arrow in the merged images. (E) The GFP-Ufe1:mCherry-Sec12 signal ratio in the cluster in the presence of GMP-PNP or GTP. Error bars represent s.e.m. (GMP-PNP, n=6; GTP, n=7). Scale bars: 2 µm.

the protein components of the COPII machinery during their polymerization into a two-dimensional lattice on the membrane.

Although Sec23-induced GTP hydrolysis is necessary for Sar1 release from the membrane and the subsequent COPII uncoating of the vesicles to allow fusion with the target membrane, it has long been unclear at which time point Sar1 and the COPII coat dissociate from the membrane during the COPII-budding process. Based on our finding that Sar1 molecules are predominantly distributed at the edge of the COPII–cargo cluster under GTP-hydrolyzing conditions (Fig. 2), Sar1 dissociation seems to occur at the early stages of COPII coat assembly, possibly even before the vesicles pinch off from the ER membrane. This may not result in an early uncoating of the COPII coat as we also showed that the outer coat complex Sec13–Sec31 remains bound to the cargo cluster despite Sar1 dissociation. Our data are in agreement with a recent live-cell imaging study in *S. cerevisiae* cells, suggesting that Sar1 localizes at the rim of the COPII-coated areas of the ER membrane (Kurokawa et al., 2016). Although we could not directly visualize the inner coat subunits Sec23–Sec24, the fact that the Sec23 subunit provides the binding scaffold for Sec31 (Bi et al., 2007) leads to the assumption that the Sec23–Sec24 complex is also included throughout the COPII–cargo cluster even under GTP-hydrolyzing conditions.

Journal of Cell Science (2017) 130, 2893-2902 doi:10.1242/jcs.203844

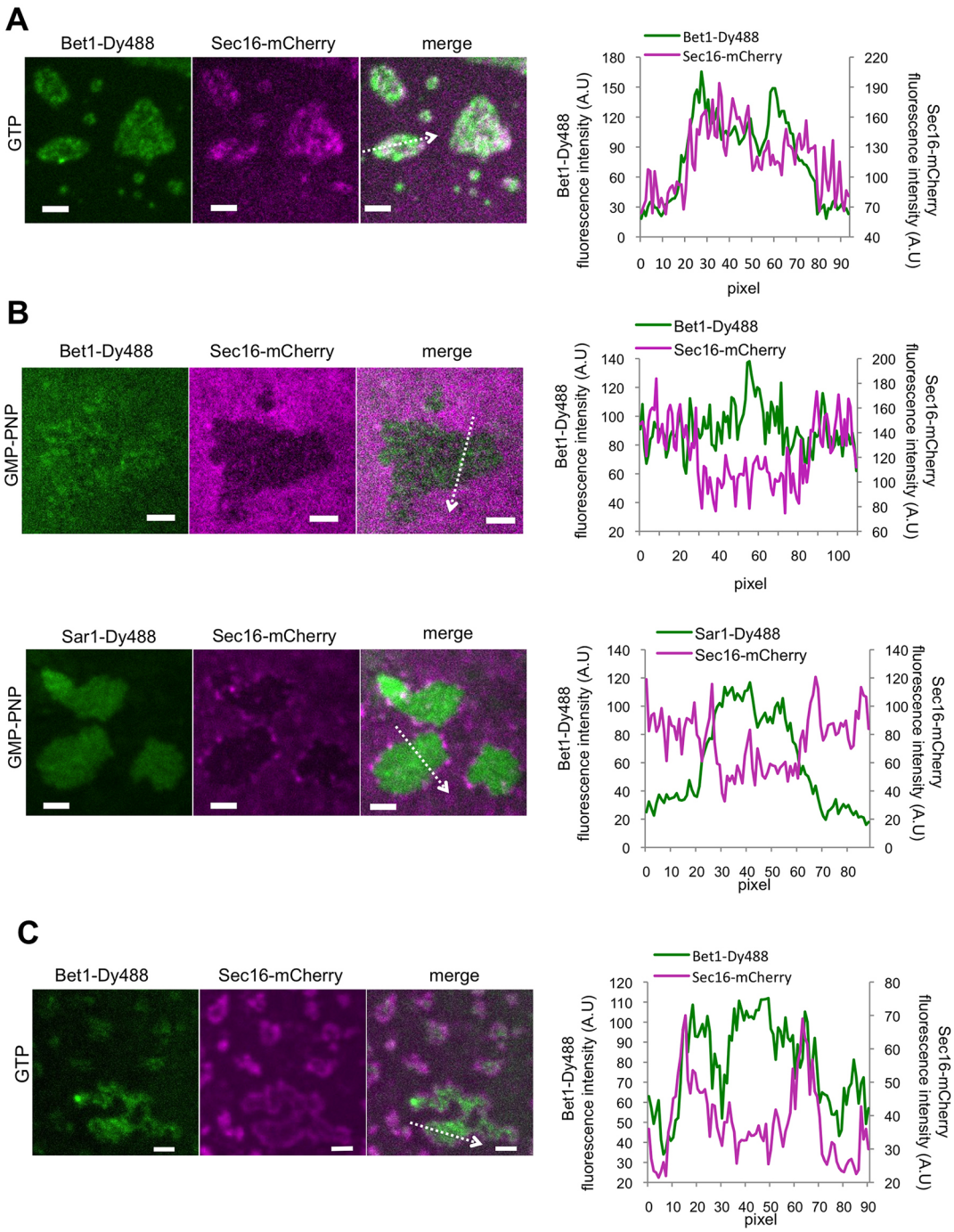

Fig. 5. Distribution of Sec16 during COPII–cargo cluster formation. (A) The colocalization of Bet1–Dy488 and Sec16–mCherry in the clusters formed in the presence of GTP. COPII components (100 ng Sar1, 380 ng Sec23–Sec24 and 1.3 µg Sec13–Sec31) and Sec16–mCherry (93.6 ng) were added to the membrane reconstituted with Bet1–Dy488 and Sec12Δlum. (B) The colocalization of Sec16–mCherry and Bet1–Dy488 or Sar1–Dy488 in the clusters formed in the presence of GMP-PNP. COPII components (100 ng Sar1 or 86 ng Sar1–Dy488, 380 ng Sec23–Sec24 and 1.3 µg Sec13–Sec31) and Sec16–mCherry (93.6 ng) were added to the membrane reconstituted with Bet1 and Sec12Δlum. Fluorescence images were taken under a confocal microscope. Dy488 and mCherry fluorescence channels, and merged images are shown. (C) The colocalization of Bet1–Dy488 and Sec16–mCherry in the clusters formed in the presence of GTP as in A, except that Sec16–mCherry was added exogenously to preformed COPII–Bet1–Dy488 clusters. COPII components (100 ng Sar1, 690 ng Sec23–Sec24 and 1.9 µg Sec13–Sec31) were added to the membrane reconstituted with Bet1–Dy488 and Sec12Δlum. After a 10-min incubation period to allow COPII–cargo cluster formation Sec16–mCherry (124.8 ng) was added and incubation continued for an additional 1 min. Fluorescence images were taken under a confocal microscope. Dy488 and mCherry fluorescence channels, and merged images are shown. Right panels show the line-scan quantification of the fluorescent signal at the position indicated by the dashed arrow in the merged image. Scale bars: 2 µm.

Associations of inner COPII coat subunit Sec24 with cargo proteins are shown to be of rather low affinity (Mossessova et al., 2003), which is in agreement with the transient nature of Sec23–Sec24 binding to transmembrane cargo in the absence of repeated cycles of Sec12-dependent GTP loading of Sar1 (Sato and Nakano, 2005b). However, we showed here that once the complete COPII coat

Journal of Cell Science (2017) 130, 2893-2902 doi:10.1242/jcs.203844

structure (containing both Sec23–Sec24 and Sec13–Sec31 complexes) has been formed on the membrane, Sar1 is no longer required to maintain the COPII coat structure (Fig. 3). These possibilities, and our data, are consistent with previous findings showing that COPII vesicles generated *in vitro* in the presence of GTP contain almost no Sar1 but remain coated (Barlowe et al., 1994). The COPII coat binds to the membrane during vesicle formation, but it needs to be dissociated before vesicle fusion to allow exposure of fusogenic machinery. This suggests that additional layers of regulation, other than Sar1 GTP hydrolysis, may exist to drive uncoating. Recent data indicate that phosphorylation of coat subunits (Sec23 and Sec31) is part of such an uncoating mechanism (Lord et al., 2011).

We previously demonstrated that the minimal COPII machinery can efficiently exclude non-cargo transmembrane proteins from cargo clusters, and the efficiency of exclusion is facilitated by Sar1 GTPase cycles (Tabata et al., 2009). We reasoned that this is because densely packed prebudding complexes clustered by Sec13–Sec31 may form a structural barrier against the incorporation of proteins without export signals into the clusters. Indeed, we observed that the non-cargo protein Sec12 is efficiently excluded from cargo clusters. However, the efficiency of the exclusion is not markedly affected by the presence of GTP or GMP-PNP (Fig. 4). Although the reason underlying this GTPase independence is not currently clear, it may be related to the fact that Sec12 is not simply a non-cargo protein but is directly involved in COPII coat assembly by interacting with Sar1.

Even though addition of purified Sec23–Sec24, Sec13–Sec31, and GTP-locked Sar1 to synthetic liposomes is sufficient to generate small vesicles, the presence of Sec16 stimulates vesicle formation (Supek et al., 2002). Therefore, Sec16 has been proposed to contribute to the COPII coat recruitment. In fact, it has been shown that there are distinct binding sites on Sec16 for each COPII subunit, and it has been suggested that Sec16 may act on the ER membrane to facilitate COPII coat assembly (Gimeno et al., 1996; Shaywitz et al., 1997; Yorimitsu and Sato, 2012). However, we did not observe any apparent alterations in the formation and appearance of COPII–cargo clusters generated in the presence of Sec16–mCherry or a non-labeled Sec16 (i.e. without mCherry fusion at its C-terminus) (Fig. S1). As our imaging system does not have sufficient time resolution to trace the cluster growth dynamics, it is possible that Sec16 affects the very early stage of COPII assembly. Instead, we showed that Sec16 molecules are efficiently incorporated into the COPII–cargo clusters (Fig. 5). This result provides important clues as to whether Sec16 is packaged into the COPII vesicles or not. Sec16 has been found in COPII vesicles (or tubulovesicular membranes) in *S. cerevisiae* (Espenshade et al., 1995), *Drosophila* (Ivan et al., 2008) and humans (Hughes et al., 2009), but it seems to be present at a significantly lower stoichiometry relative to COPII subunits (Connerly et al., 2005). Our experimental system is able to reproduce both efficient cargo concentration and non-cargo exclusion (Tabata et al., 2009); therefore, the specific incorporation of Sec16 into the COPII–cargo clusters has an important implication. Thus, even if the packaging of Sec16 into COPII vesicles is very low, our results imply that it may not represent non-specific incorporation. We sought to obtain mechanistic insights into how the large Sec16 protein (~2000 residues) fitted into the densely packed COPII assembly. In the case of the Sec16 family proteins, the long highly disordered regions surrounding the structured domains (~400 residues, known as the 'central conserved domain') are well conserved in various species (Whittle and Schwartz, 2010; Pietrosemoli et al., 2013). Thus, the entire Sec16 protein need not be localized to the membrane-proximal region of the COPII lattice; for example, these disordered regions can be accommodated within the membrane-distal part of the COPII coat structure. We have previously shown that when purified Sec16–mOrange alone was added onto the planar membrane, dispersed fluorescent spots that represent uniformly self-assembled Sec16–mOrange were observed by TIRF microscopy (Yorimitsu and Sato, 2012). However, when observed with the complete set of COPII components, we demonstrated that Sec16 molecules are distributed fairly uniformly throughout the COPII–cargo clusters (Fig. 5A). This may be due to the presence of COPII coat and Sar1, which may act to alter the self-assembled state of Sec16.

Surprisingly, when GTP-locked Sar1 was used to generate COPII–cargo clusters, Sec16 molecules were predominantly excluded from

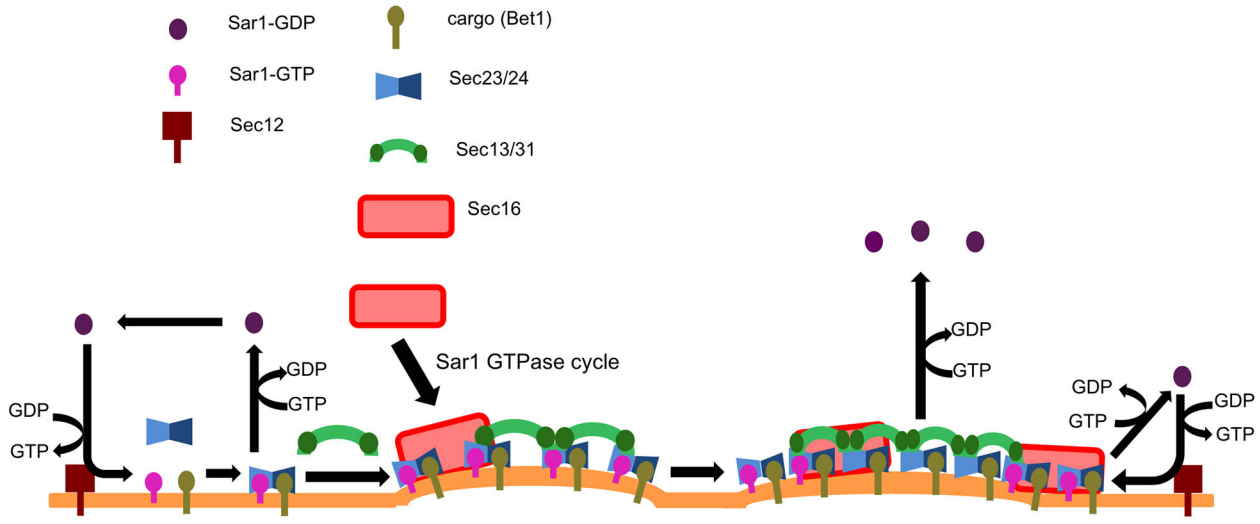

Fig. 6. Model summarizing the COPII coat polymerization. The COPII coat polymerization is initiated by the GDP/GTP exchange on Sar1 by its GEF, Sec12. Activated Sar1-GTP binds to the ER membrane and the cytoplasmically exposed signal of transmembrane cargo is captured by Sec23–Sec24, forming the prebudding complex. The prebudding complexes are clustered by Sec13–Sec31. During this process, Sec16 molecules are possibly incorporated into the COPII–cargo clusters. Although it is currently not clear whether a fraction of Sec16 is incorporated into COPII-coated carriers, the two-dimensional COPII coat lattice is sterically able to accommodate and retain Sec16 molecules.

Journal of Cell Science

the clusters (Fig. 5B). It is not immediately clear exactly how the Sar1 GTPase contributes to the incorporation of Sec16 and why the absence of the Sar1 GTPase cycle leads to the exclusion of Sec16. One possibility is that the presence of membrane-bound Sar1 in the COPII–cargo cluster sterically hinders the incorporation of Sec16. An alternative possibility is that in the absence of the Sar1 GTPase cycle, Sec16 does not participate in COPII coat polymerization and is thus not actively concentrated into the COPII–cargo cluster. This is in line with *in vitro* experiments where the stimulation of COPII budding efficiency by Sec16 is dependent only on GTP (Supek et al., 2002). Moreover, our results raise the possibility that additional levels of regulation may exist between Sar1 GTPase and Sec16 function (Fig. 6).

It has been proposed that *Pichia pastoris* Sec16 acts at the edges of the COPII assembly (Bharucha et al., 2013), and a very recent study in *Drosophila*, using super-resolution fluorescence microscopy, demonstrated that Sec16 is present as rings around the edges of the polymerized COPII structures (Liu et al., 2017). Although it is uncertain whether *S. cerevisiae* Sec16 localizes at the rims of COPII-coated membranes in living cells, Sec16 is known to localize to the concave cup-shaped structures of the ER membrane in *Drosophila* and mammalian cells (Ivan et al., 2008; Budnik and Stephens, 2009; Hughes et al., 2009). It remains unclear whether Sec16 has a direct role in generating this curved membrane structure, or the curvature itself is required for efficient Sec16 localization. In either case, because the model membrane used in this study is highly resistant to bending to avoid vesicle fission, it may restrict mechanical deformation of the membrane required to drive ERES formation. For this reason, our results demonstrating that Sec16 exists throughout the COPII assembly may not reflect its physiological functions at the ERES. Nevertheless, the present results do suggest that the two-dimensional COPII coat lattice is capable of accommodating Sec16, which emphasizes the need to consider the possible inclusion of Sec16 within the assembling COPII coat.

MATERIALS AND METHODS

Plasmid construction

Two tandem repeats of the Strep tag followed by an mOrange tag and the N-terminal domain of Sec12 (residues 1–373) without the luminal domain (Sec12Δlum) were generated by PCR from pmOrange (Clontech) and pKSE176 (Sato and Nakano, 2005b), then inserted into the *Eco*RI-*Xho*I sites of pPR-IBA2 (IBA), which codes for 2Strep-mOrange-Sec12Δlum (mOrange–Sec12), yielding the plasmid pKSE290. The plasmid pIBA2-2Strep-mOrange-Sec12Δlum encoding 2Strep-mCherry-Sec12Δlum (mCherry–Sec12) was constructed in the same way as pKSE290 except that the mCherry portion was amplified from pmCherry (Clontech). The coding sequence for EGFP was amplified by PCR from pEGFP-1 (Clontech) and inserted into the *Bam*HI site of pKSE136 (Sato and Nakano, 2004) to yield pKSE232 (MBP–GFP–Ufe1). The DNA fragment coding for mCherry was inserted into the *Bam*HI-*Xho*I sites of pTYY41 (Yorimitsu and Sato, 2012), which codes for Sec16–mCherry, yielding the plasmid pSec16-mCherry(314). The *Sph*I-*Xho*I fragment of pSec16-mCherry(314) was inserted into the *Sph*I-*Xho*I sites of pCUP1-MBP-Sec16-mOrange (Yorimitsu and Sato, 2012), which codes for MBP–Sec16–mCherry, to yield the pCUP1-MBP-Sec16-mCherry. The coding sequence for Sar1 was generated by PCR from pMYE3-1 (Saito et al., 1998) and inserted into the *Bam*HI-*Sal*I sites of pGEX-4T-1 (GE Healthcare). An *Eco*RI site was created just before the stop codon in the above plasmid and the fragment encoding the mCherry and the stop codon was inserted into the *Eco*RI-*Sal*I sites to yield pKSE288 (GST–Sar1–mCherry).

Protein preparation and fluorescent labeling

Sar1, Sec23–Sec24, and Sec13–Sec31 were prepared as described previously (Sato and Nakano, 2005b). Strep-tagged Bet1 and Sec12Δlum were expressed and purified as described previously (Tabata et al., 2009). Strep-tagged mOrange–Sec12 and mCherry–Sec12 were purified with the same protocol used for Sec12Δlum. MBP–GFP–Ufe1 was purified as previously described (Sato and Nakano, 2004). Sar1–mCherry was prepared from GST–Sar1–mCherry using the same procedure as for Sar1p-C171S-Cys (Tabata et al., 2009). Sec16–mCherry was purified in the same way as was Sec16–mOrange (Yorimitsu and Sato, 2012). The site-directed fluorescent labeling of Sar1 and Bet1 by Cy3–maleimide (GE Healthcare) or DyLight488–maleimide (Thermo Scientific) was performed as previously described (Tabata et al., 2009). Sec13/31–Cy3 and Sec13/31–ATTORho101 were prepared by reacting purified Sec13–Sec31 (in 20 mM HEPES-KOH, pH 7.4, 175 mM KOAc, 0.1 mM EDTA, and 10% glycerol) with an ∼60-fold molar excess Cy3–maleimide or ATTORho101–maleimide (ATTO TEC), respectively, followed by removal of excess (nonreacted) reagent with a NAP-5 desalting column (GE Healthcare). The labeling efficiency was approximately 1.9–2.9 (dye:protein ratio).

Preparation of proteoliposomes

Proteoliposomes were prepared from the major–minor mix lipid formulation (Matsuoka et al., 1998) as described previously (Tabata et al., 2009).

Microscopy

The fluorescently labeled proteins in the artificial lipid bilayer were imaged at room temperature using an objective-type total internal reflection fluorescence (TIRF) microscope or laser scanning confocal microscope based on an Olympus IX71 inverted microscope with an electron multiplying charge-coupled device camera (iXon, DU897, Andor Technology). An oil immersion objective lens (PlanApo, ×100, 1.45 NA) was located just below the lower chamber. For TIRF imaging, bilayers were illuminated by an evanescent wave with a 532 nm solid-state laser (COMPASS 215M-75, Coherent) as described previously (Tabata et al., 2009). Confocal imaging was carried out with a CSU10 spinning-disk confocal scanner (Yokogawa Electric Corporation). In this setting, a 473 nm solid-state laser (J050BS, Showa Optronics) was used to excite GFP and DyLight488 and a 561 nm solid-state laser (J050YS, Showa Optronics) was used to excite mCherry and ATTORho101. The acquired images were analyzed using Andor iQ (Andor Technology) and ImageJ software (NIH).

Formation of horizontal lipid bilayers and protein incorporation

Artificial lipid bilayers were formed horizontally by placing the major-minor lipid mix dissolved in n-decane at the hole of the lab-made upper chamber as previously described (Tabata et al., 2009). Proteoliposomes reconstituted separately with Sec12Δlum (120–140 μg ml^{-1}), mOrange–Sec12 (630 μg ml^{-1}), mCherry–Sec12 (720 μg ml^{-1}), Bet1 (100–220 μg ml^{-1}), Bet1–Dy488 (70–240 μg ml^{-1}), and GFP–Ufe1 (224 μg ml^{-1}) were diluted with buffer (between 1.5- and 10,000-fold) containing 20 mM HEPES-KOH, pH 6.8, 150 mM KOAc, 2 mM $MgCl_2$, 5% (v/v) glycerol, and 0.2 mM GTP or GMP-PNP. This solution was then added from the upper chamber onto the bilayer membrane where they fused spontaneously with the bilayer membrane. After a 10-min incubation to allow membrane fusion, excess proteoliposomes were withdrawn using a glass pipet. As 80–95% of the cytoplasmic domains of Bet1 and Sec12Δlum were oriented on the outside of the liposomes (Sato and Nakano, 2005a), an equal proportion of these domains of the bilayer-reconstituted Bet1 and Sec12Δlum should be exposed to the upper surface of the bilayer membrane.

Observation of fluorescently labeled proteins in the bilayer membrane

All experiments were performed at room temperature. The upper chamber was placed upward from the coverslip, where the distance between the bilayer and the coverslip was ∼10–20 μm to position both sides of the membrane in an aqueous environment. COPII components [∼10 μl of the mixture containing 40–100 ng Sar1 (or labeled Sar1), 345–690 ng Sec23–Sec24, and 1.3–1.9 μg Sec13–Sec31 (or labeled Sec13/31)] were added from the upper chamber (total ∼400 μl) to the bilayer membrane formed in an aqueous environment reconstituted with Bet1 and Sec12. In some cases, 62–125 ng of Sec16–mCherry (or non-labeled Sec16) was also included. The chamber solution contained 20 mM HEPES-KOH pH 6.8, 150 mM

KOAc, 2 mM $MgCl_2$, and 0.2 mM GTP or GMP-PNP. After 10–20 min incubation, the bilayer membrane was then attached to the coverslip. Fluorescence images were taken under a TIRF or confocal microscope. Sec13/31–ATTORho101 was mixed at a 1:4 molar ratio with unlabeled Sec13–Sec31. The histograms in Figs 2E and 3D were fitted to a Gaussian curve $y=A\times exp-(x-B)^2/C^2$, where the parameter A is the height of the peak, B is the center value, and C is the width of the peak.

Acknowledgements
We are grateful to the members of the Sato laboratory for helpful discussions.

Competing interests
The authors declare no competing or financial interests.

Author contributions
Conceptualization: H.I., K.S.; Methodology: H.I., K.S.; Validation: H.I.; Formal analysis: H.I., K.S.; Investigation: H.I., T.Y., K.S.; Resources: H.I., T.Y., K.S.; Data curation: H.I., K.S.; Writing - original draft: H.I.; Writing - review & editing: T.Y., K.S.; Supervision: K.S.; Project administration: K.S.; Funding acquisition: K.S.

Funding
This work was supported in part by the Grant-in-Aid for Scientific Research (C) and the Grant-in-Aid for Scientific Research on Innovation Areas 'Dynamical ordering of biomolecular systems for creation of integrated functions' from the Japanese Ministry of Education, Culture, Sports, Science and Technology. This work was also supported by the Naito Foundation, the Takeda Science Foundation, and The Precise Measurement Technology Promotion Foundation.

Supplementary information
Supplementary information available online at
http://jcs.biologists.org/lookup/doi/10.1242/jcs.203844.supplemental

References
Antonny, B., Madden, D., Hamamoto, S., Orci, L. and Schekman, R. (2001). Dynamics of the COPII coat with GTP and stable analogues. *Nat. Cell Biol.* **3**, 531-537.
Bannykh, S. I., Rowe, T. and Balch, W. E. (1996). The organization of endoplasmic reticulum export complexes. *J. Cell Biol.* **135**, 19-35.
Barlowe, C. K. and Miller, E. A. (2013). Secretory protein biogenesis and traffic in the early secretory pathway. *Genetics* **193**, 383-410.
Barlowe, C. and Schekman, R. (1993). SEC12 encodes a guanine-nucleotide-exchange factor essential for transport vesicle budding from the ER. *Nature* **365**, 347-349.
Barlowe, C., Orci, L., Yeung, T., Hosobuchi, M., Hamamoto, S., Salama, N., Rexach, M. F., Ravazzola, M., Amherdt, M. and Schekman, R. (1994). COPII: a membrane coat formed by Sec proteins that drive vesicle budding from the endoplasmic reticulum. *Cell* **77**, 895-907.
Bharucha, N., Liu, Y., Papanikou, E., McMahon, C., Esaki, M., Jeffrey, P. D., Hughson, F. M. and Glick, B. S. (2013). Sec16 influences transitional ER sites by regulating rather than organizing COPII. *Mol. Biol. Cell* **24**, 3406-3419.
Bhattacharyya, D. and Glick, B. S. (2007). Two mammalian Sec16 homologues have nonredundant functions in endoplasmic reticulum (ER) export and transitional ER organization. *Mol. Biol. Cell* **18**, 839-849.
Bi, X., Corpina, R. A. and Goldberg, J. (2002). Structure of the Sec23/24-Sar1 pre-budding complex of the COPII vesicle coat. *Nature* **419**, 271-277.
Bi, X., Mancias, J. D. and Goldberg, J. (2007). Insights into COPII coat nucleation from the structure of Sec23.Sar1 complexed with the active fragment of Sec31. *Dev. Cell* **13**, 635-645.
Budnik, A. and Stephens, D. J. (2009). ER exit sites–localization and control of COPII vesicle formation. *FEBS Lett.* **583**, 3796-3803.
Connerly, P. L., Esaki, M., Montegna, E. A., Strongin, D. E., Levi, S., Soderholm, J. and Glick, B. S. (2005). Sec16 is a determinant of transitional ER organization. *Curr. Biol.* **15**, 1439-1447.
D'Arcangelo, J. G., Stahmer, K. R. and Miller, E. A. (2013). Vesicle-mediated export from the ER: COPII coat function and regulation. *Biochim. Biophys. Acta* **1833**, 2464-2472.
Espenshade, P., Gimeno, R. E., Holzmacher, E., Teung, P. and Kaiser, C. A. (1995). Yeast SEC16 gene encodes a multidomain vesicle coat protein that interacts with Sec23p. *J. Cell Biol.* **131**, 311-324.
Fath, S., Mancias, J. D., Bi, X. and Goldberg, J. (2007). Structure and organization of coat proteins in the COPII cage. *Cell* **129**, 1325-1336.
Gimeno, R. E., Espenshade, P. and Kaiser, C. A. (1996). COPII coat subunit interactions: Sec24p and Sec23p bind to adjacent regions of Sec16p. *Mol. Biol. Cell* **7**, 1815-1823.
Huang, M., Weissman, J. T., Beraud-Dufour, S., Luan, P., Wang, C., Chen, W., Aridor, M., Wilson, I. A. and Balch, W. E. (2001). Crystal structure of Sar1-GDP at 1.7 A resolution and the role of the NH2 terminus in ER export. *J. Cell Biol.* **155**, 937-948.
Hughes, H., Budnik, A., Schmidt, K., Palmer, K. J., Mantell, J., Noakes, C., Johnson, A., Carter, D. A., Verkade, P., Watson, P. et al. (2009). Organisation of human ER-exit sites: requirements for the localisation of Sec16 to transitional ER. *J. Cell Sci.* **122**, 2924-2934.
Ivan, V., de Voer, G., Xanthakis, D., Spoorendonk, K. M., Kondylis, V. and Rabouille, C. (2008). Drosophila Sec16 mediates the biogenesis of tER sites upstream of Sar1 through an arginine-rich motif. *Mol. Biol. Cell* **19**, 4352-4365.
Iwasaki, H., Yorimitsu, T. and Sato, K. (2015). Distribution of Sec24 isoforms to each ER exit site is dynamically regulated in Saccharomyces cerevisiae. *FEBS Lett.* **589**, 1234-1239.
Kung, L. F., Pagant, S., Futai, E., D'Arcangelo, J. G., Buchanan, R., Dittmar, J. C., Reid, R. J. D., Rothstein, R., Hamamoto, S., Snapp, E. L. et al. (2012). Sec24p and Sec16p cooperate to regulate the GTP cycle of the COPII coat. *EMBO J.* **31**, 1014-1027.
Kurokawa, K., Suda, Y. and Nakano, A. (2016). Sar1 localizes at the rims of COPII-coated membranes in vivo. *J. Cell Sci.* **129**, 3231-3237.
Liu, M., Feng, Z., Ke, H., Liu, Y., Sun, T., Dai, J., Cui, W. and Pastor-Pareja, J. C. (2017). Tango1 spatially organizes ER exit sites to control ER export. *J. Cell Biol.* **216**, 1035-1049.
Lord, C., Bhandari, D., Menon, S., Ghassemian, M., Nycz, D., Hay, J., Ghosh, P. and Ferro-Novick, S. (2011). Sequential interactions with Sec23 control the direction of vesicle traffic. *Nature* **473**, 181-186.
Matsuoka, K., Orci, L., Amherdt, M., Bednarek, S. Y., Hamamoto, S., Schekman, R. and Yeung, T. (1998). COPII-coated vesicle formation reconstituted with purified coat proteins and chemically defined liposomes. *Cell* **93**, 263-275.
Miller, E., Antonny, B., Hamamoto, S. and Schekman, R. (2002). Cargo selection into COPII vesicles is driven by the Sec24p subunit. *EMBO J.* **21**, 6105-6113.
Miller, E. A., Beilharz, T. H., Malkus, P. N., Lee, M. C. S., Hamamoto, S., Orci, L. and Schekman, R. (2003). Multiple cargo binding sites on the COPII subunit Sec24p ensure capture of diverse membrane proteins into transport vesicles. *Cell* **114**, 497-509.
Mossessova, E., Bickford, L. C. and Goldberg, J. (2003). SNARE selectivity of the COPII coat. *Cell* **114**, 483-495.
Nakano, A. and Muramatsu, M. (1989). A novel GTP-binding protein, Sar1p, is involved in transport from the endoplasmic reticulum to the Golgi apparatus. *J. Cell Biol.* **109**, 2677-2691.
Oka, T., Nishikawa, S. and Nakano, A. (1991). Reconstitution of GTP-binding Sar1 protein function in ER to Golgi transport. *J. Cell Biol.* **114**, 671-679.
Orci, L., Ravazzola, M., Meda, P., Holcomb, C., Moore, H. P., Hicke, L. and Schekman, R. (1991). Mammalian Sec23p homologue is restricted to the endoplasmic reticulum transitional cytoplasm. *Proc. Natl. Acad. Sci. USA* **88**, 8611-8615.
Pietrosemoli, N., Pancsa, R. and Tompa, P. (2013). Structural disorder provides increased adaptability for vesicle trafficking pathways. *PLoS Comput. Biol.* **9**, e1003144.
Saito, Y., Kimura, K., Oka, T. and Nakano, A. (1998). Activities of mutant Sar1 proteins in guanine nucleotide binding, GTP hydrolysis, and cell-free transport from the endoplasmic reticulum to the Golgi apparatus. *J. Biochem.* **124**, 816-823.
Sato, K. and Nakano, A. (2004). Reconstitution of coat protein complex II (COPII) vesicle formation from cargo-reconstituted proteoliposomes reveals the potential role of GTP hydrolysis by Sar1p in protein sorting. *J. Biol. Chem.* **279**, 1330-1335.
Sato, K. and Nakano, A. (2005a). Reconstitution of cargo-dependent COPII coat assembly on proteoliposomes. *Methods Enzymol.* **404**, 83-94.
Sato, K. and Nakano, A. (2005b). Dissection of COPII subunit-cargo assembly and disassembly kinetics during Sar1p-GTP hydrolysis. *Nat. Struct. Mol. Biol.* **12**, 167-174.
Shaywitz, D. A., Espenshade, P. J., Gimeno, R. E. and Kaiser, C. A. (1997). COPII subunit interactions in the assembly of the vesicle coat. *J. Biol. Chem.* **272**, 25413-25416.
Shindiapina, P. and Barlowe, C. (2010). Requirements for transitional endoplasmic reticulum site structure and function in Saccharomyces cerevisiae. *Mol. Biol. Cell* **21**, 1530-1545.
Supek, F., Madden, D. T., Hamamoto, S., Orci, L. and Schekman, R. (2002). Sec16p potentiates the action of COPII proteins to bud transport vesicles. *J. Cell Biol.* **158**, 1029-1038.
Tabata, K. V., Sato, K., Ide, T., Nishizaka, T., Nakano, A. and Noji, H. (2009). Visualization of cargo concentration by COPII minimal machinery in a planar lipid membrane. *EMBO J.* **28**, 3279-3289.
Watson, P., Townley, A. K., Koka, P., Palmer, K. J. and Stephens, D. J. (2006). Sec16 defines endoplasmic reticulum exit sites and is required for secretory cargo export in mammalian cells. *Traffic* **7**, 1678-1687.
Whittle, J. R. R. and Schwartz, T. U. (2010). Structure of the Sec13-Sec16 edge element, a template for assembly of the COPII vesicle coat. *J. Cell Biol.* **190**, 347-361.
Yorimitsu, T. and Sato, K. (2012). Insights into structural and regulatory roles of Sec16 in COPII vesicle formation at ER exit sites. *Mol. Biol. Cell* **23**, 2930-2942.
Yoshihisa, T., Barlowe, C. and Schekman, R. (1993). Requirement for a GTPase-activating protein in vesicle budding from the endoplasmic reticulum. *Science* **259**, 1466-1468.